Modeling and main parameters identification of an absorption chiller, experimental validation.

Julien Heintz[1], Nabil Benabdelmoumene[1], Guillaume Anies[2], Stephane Gibout[2], Erwin Franquet[2] and Jean Castaing-Lasvignottes[2*]

[1] CETIAT, Domaine Scientifique de la Doua, 25 avenue des Arts, BP2042, 69603 Villeurbanne Cedex France

[2] Laboratoire de Thermique, Energetique et Procédés. Université de Pau et Pays de l'Adour 64000 Pau France

[*] Corresponding Author, jean.castaing@univ-pau.fr

Abstract

The liquid absorption tri-thermal refrigeration systems are particularly promising for solar cooling. Designed and sized in order to reply to nominal conditions, these machines are often submitted to varying operating conditions (cooling load, temperature and flow). The influence of these changes on the machine behavior and the associated energy performance are rather tricky to predict. The numerical simulation of the system is an alternative to experimentation and systematic analysis on pilot. But a good knowledge of the main parameters which characterize the simulated machine is necessary. As the performances are directly related to temperature levels, various experimental conditions were applied to a particular solar absorption chiller: a SCHÜCO LB of 15 kW.

After a brief review of the operating principle, the experimental results obtained on a test bench are presented. In a second step, a model is developed to predict the chiller's performance based on operating temperatures. An identification tools is realized to identify the design parameters of the chiller thanks to three steady states tests. Finally, the model is validated on other experimental results.

1. Introduction

The worldwide development reduces fossil energy sources. Energy production, industries, transport, agriculture, building generate greenhouse gases emissions leading to the climate change. In consequence, a rise of an average annual daily temperature between 1.4°C and 5.8°C by 2100 is expected [1]. In parallel, the thermal comfort demand in summer increases in the residential: 30 millions of air conditioned m² installed in 1980 to over 150 millions in 2000 [2, 3]. Due to this problematic and to the correlation between chilling charge and solar energy source, a lot of studies are realized to find the most sustainable solutions for solar air conditioning [4]. Different systems exist such as desiccant liquid, desiccant rotor, adsorption, absorption … but only experimental pilots represent the majority of installed systems [5, 6, 7 and 8]. There are about 70 solar installations in Europe and absorption chiller represents 60% [9 and 10]. These tri-thermal machines can produce chilled water at 10-12°C thanks to a hot source at 80-90°C. These temperature levels are compatible with solar energy utilization (flat plates or evacuated tubes collectors) [11]. Many works have demonstrated the interest of such systems [12] but there is still a need for R&D in order to develop and to improve reliability of components, conception, regulation and implementation. The absorption principle is the most developed and is explained by a most mature technology often used with waste heat or combustion. In the solar air conditioning case, the market is under development and many manufacturers propose some products (EAW, ROTARTICA, YAZAKI SONNENKLIMA, …) [13].

The research's project ABCLIMSOL (Program ANR PREBAT 2007) is making up several partners (EDF R&D, CETIAT, CEA INES, LATEP, CETHIL) charged in particular to assess the performance of different absorption chillers in real or simulated solar operating conditions. EDF R&D has already tested a ROTARTICA solar 045 chiller [14]. This works enabled to detail the behavior and the performances of this chiller in comparison to Izquierdo [15], Rodriguez Hidalgo [16] and Agyenim [17] thanks to imposed known working conditions.

Modeling such an absorption chiller requires the knowledge of the main different design parameters of the machine (UA factor of the heat exchangers, volume flow rate of the diluted solution and thermal efficiency of the internal heat exchanger) and sometimes there are difficult to estimate. To evaluate these characteristics, an identification procedure has been set up and this document explains the used method to model a SCHÜCO LB 15 chiller.

In a first part, the absorption principle is recalled and the performances are introduce with the balance equations of energy and mass associated to each component (condenser, evaporator, absorber and generator). Secondly, the test bench and the followed protocol are described. The experimental results in steady states and their analyses are presented. The nominal and no-nominal operating areas are identified and experimental results discussed. The next part talks about the modeling and the simulation of such a machine, considering thermodynamic properties of the cycle as well as technological integration of the heat exchangers. Then, the identification procedure and the results are presented, concluding to a quite accurate methodology since simulated results are in good agreement with the experiments.

2. Operating principle and performances

The absorption chillers are tri-thermal machines. They work thanks to three levels of temperature $T_l<T_m<T_h$. Both temperature T_m and T_l imply respectively two levels of pressure, a high pressure P_h (in the condenser and the desorber) and a low pressure P_l (in the evaporator and the absorber).They produce only cold from a heat supply at the temperature T_h, i.e. without work exchange with the outside. The absorption chillers uses the capability of some liquid, to absorb (exothermic reaction) and to desorb (endothermic reaction) a refrigerant steam. The solubility of the vapor in the liquid depends on the temperature and the pressure. Thus, these machines use as working fluid a binary mixture, whose one is much more volatile than the other and constitutes the refrigerant. The mainly used couple in solar absorption chiller is Water + Lithium Bromide (H_2O/LiBr), the water being the refrigerant. The figure 1 shows a single effect absorption chiller and its main components. On a single effect chiller, two mass balances can be written, one relative to the total mass flow rate, another to the LiBr mass flow rate:

$$\begin{cases} \dot{m} + \dot{c} = \dot{d} \\ x_c \cdot \dot{c} = x_d \cdot \dot{d} \end{cases} \tag{1}$$

An energy balance is written for each component and the following equation system is obtained:

$$\begin{cases} \text{Desorber}: \dot{Q}_{desorb} = \dot{m} \cdot h_7 + \dot{c} \cdot h_6 - \dot{d} \cdot h_5 \\ \text{Condenser}: \dot{Q}_{cond} = \dot{m} \cdot (h_1 - h_7) \\ \text{Evaporator}: \dot{Q}_{evap} = \dot{m} \cdot (h_3 - h_2) \\ \text{Absorber}: \dot{Q}_{abs} = \dot{d} \cdot h_4 - \dot{m} \cdot h_3 - \dot{d} \cdot h_8 \\ \text{Pump}: \dot{W}_{pump} = \dot{d} \cdot (h_{4'} - h_4) \end{cases} \tag{2}$$

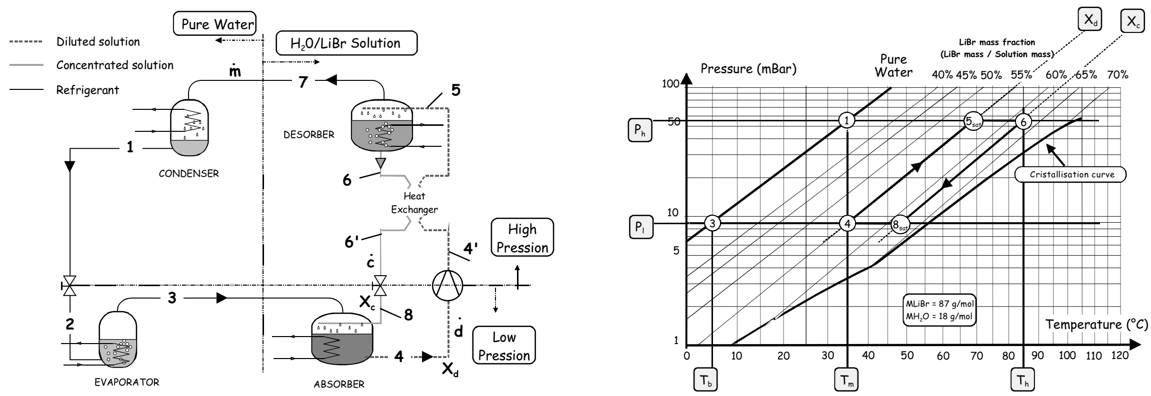

Fig.1 Sketch of a H_2O/LiBr single effect absorption chiller and the associated cycle in a Oldham diagram

To increase the thermal performance of the absorption chiller, an internal heat exchanger is used between the desorber and the absorber. It preheats the diluted solution and subcools the concentrated solution. Therefore to produce the same chilling capacities, the required energy input is reduced. This heat exchanger is characterized by this following thermal efficiency:

$$\varepsilon = \frac{T_{6'} - T_6}{T_{4'} - T_6} \tag{3}$$

The Coefficient Of Performance (COP) of this cycle takes the following expression:

$$COP = \frac{\dot{Q}_{evap}}{\dot{Q}_{desorb} + \dot{W}_{pump}} = \frac{(h_3 - h_2)}{\left(h_7 + \frac{x_d}{x_c - x_d} \cdot h_6 - \frac{x_c}{x_c - x_d} \cdot (h_5 + h_4 - h_{4'})\right)} \tag{4}$$

For each chiller, this value depends essentially of the cycle temperature levels (T_l, T_m and T_h). Generally for a single effect chiller, the range is between 0.6 and 0.75 from the manufacturer.

3. Experimental test bench and results

The research's project ABCLIMSOL concerns several partners (EDF R&D, CETIAT, CEA INES, LATEP, CETHIL). They are charged in particular to assess the performance of different absorption chillers in reel or simulated solar operating conditions. A SCHÜCO chiller, model LB15, has been tested at CETIAT laboratory by imposing different sets of constant sources temperature. It uses the couple H_2O/LiBr and its nominal cooling capacity is 15 kW with a COP of 0.75. The following temperature levels correspond to the manufacturer recommendation for the working range:

- Hot sources (desorber) from 70°C to 95°C
- Cooling source (absorber and condenser) from 25°C to 40°C
- Cold source (evaporator) from 6°C to 15°C

On the figure 1, the shown chiller structure is modified because the cooling loop of the absorber and the condenser are associated in series, leading to a condensation temperature slightly higher than the absorption temperature. The designed values of volumetric flow rates in the loops of the heating, cooling and chilling water are respectively of 2 m^3/h, 5 m^3/h and 1.9 m^3/h.

A test bench has been realized in order to analyze its performance. The figure 2 shows the experimental test bench of the CETIAT. The heating, cooling and chilling water loops are supplied by three controlled heat sources. Their role is to maintain a temperature at the desorber inlet, at the input of the absorber/condenser and the evaporator outlet with the imposed flow rates. To achieve the different energy balances of the installation, a data logger collects the necessary measures. To analyze the chiller performances, 27 tests were selected on the 40 tests that were conducted. This selection is composed of the working condition where the chiller works closely to its nominal performance. These latter are summarized in the table 1 and represented figure 3. This table lists for each of these tests:

- The measured temperatures corresponding to the loops of hot, cooling and cold water,
- The associated powers and the overall COP of the chiller.

Table 1: summary of different working configurations tested on the chiller

Essai	**$T_{sortie\ evap}$ [°C]**	**$T_{entrée\ abs/cond}$ [°C]**	**$T_{entrée\ desorb}$ [°C]**	**Qevap [kW]**	**Qabs_cond [kW]**	**Qdes [kW]**	**COP**
nominal	11.0 +/- 0.1	30.0 +/- 0.1	90.3 +/- 0.1	18.01 +/- 0.63	-45.17 +/- 1.60	27.58 +/- 0.72	0.65 +/- 0.04
A	6.1 +/- 0.1	30.0 +/- 0.1	89.8 +/- 0.1	12.76 +/- 0.58	-34.59 +/- 1.50	22.09 +/- 0.68	0.58 +/- 0.05
B	5.9 +/- 0.1	25.0 +/- 0.1	90.0 +/- 0.1	17.82 +/- 0.63	-47.35 +/- 1.64	28.79 +/- 0.74	0.62 +/- 0.04
C	10.0 +/- 0.1	35.0 +/- 0.1	89.7 +/- 0.1	10.00 +/- 0.55	-28.18 +/- 1.43	18.71 +/- 0.64	0.53 +/- 0.05
D	15.0 +/- 0.1	35.0 +/- 0.1	90.0 +/- 0.1	15.17 +/- 0.60	-38.87 +/- 1.54	24.10 +/- 0.69	0.63 +/- 0.04
E	14.9 +/- 0.1	40.0 +/- 0.1	90.1 +/- 0.1	8.92 +/- 0.54	-25.05 +/- 1.41	16.83 +/- 0.63	0.53 +/- 0.05
F	6.0 +/- 0.1	30.0 +/- 0.1	93.0 +/- 0.1	13.84 +/- 0.59	-38.18 +/- 1.55	24.16 +/- 0.69	0.57 +/- 0.04
G	10.1 +/- 0.1	30.0 +/- 0.1	91.1 +/- 0.1	17.03 +/- 0.62	-44.57 +/- 1.61	27.20 +/- 0.73	0.63 +/- 0.04
H	9.9 +/- 0.1	35.0 +/- 0.1	93.6 +/- 0.1	11.94 +/- 0.57	-33.44 +/- 1.50	21.53 +/- 0.67	0.55 +/- 0.04
I	15.0 +/- 0.1	35.0 +/- 0.1	91.9 +/- 0.1	16.08 +/- 0.61	-42.35 +/- 1.59	26.02 +/- 0.73	0.62 +/- 0.04
J	10.0 +/- 0.1	30.0 +/- 0.1	79.8 +/- 0.1	12.54 +/- 0.58	-33.17 +/- 1.50	20.72 +/- 0.68	0.61 +/- 0.05
K	15.0 +/- 0.1	30.0 +/- 0.1	80.1 +/- 0.1	17.56 +/- 0.63	-43.40 +/- 1.60	25.76 +/- 0.73	0.68 +/- 0.04
L	5.9 +/- 0.1	25.0 +/- 0.1	80.5 +/- 0.1	14.22 +/- 0.59	-38.38 +/- 1.55	23.21 +/- 0.69	0.61 +/- 0.04
M	10.0 +/- 0.1	25.0 +/- 0.1	80.5 +/- 0.1	18.45 +/- 0.64	-46.93 +/- 1.64	27.76 +/- 0.74	0.66 +/- 0.04
N	15.0 +/- 0.1	35.0 +/- 0.1	79.8 +/- 0.1	9.94 +/- 0.55	-27.38 +/- 1.44	17.66 +/- 0.64	0.56 +/- 0.05
O	10.1 +/- 0.1	30.0 +/- 0.1	69.4 +/- 0.1	7.34 +/- 0.53	-20.92 +/- 1.38	13.63 +/- 0.61	0.54 +/- 0.07
P	15.0 +/- 0.1	30.0 +/- 0.1	69.8 +/- 0.1	12.00 +/- 0.57	-30.61 +/- 1.47	18.46 +/- 0.66	0.65 +/- 0.06
Q	6.0 +/- 0.1	25.0 +/- 0.1	70.5 +/- 0.1	9.94 +/- 0.55	-28.02 +/- 1.45	17.23 +/- 0.63	0.58 +/- 0.05
R	10.1 +/- 0.1	25.0 +/- 0.1	70.5 +/- 0.1	14.34 +/- 0.59	-36.94 +/- 1.54	21.87 +/- 0.70	0.66 +/- 0.05
S	15.0 +/- 0.1	25.0 +/- 0.1	70.5 +/- 0.1	18.04 +/- 0.63	-45.28 +/- 1.62	26.15 +/- 0.72	0.69 +/- 0.04
T	6.0 +/- 0.1	30.0 +/- 0.1	84.5 +/- 0.1	10.75 +/- 0.56	-30.34 +/- 1.47	19.47 +/- 0.65	0.55 +/- 0.05
U	9.9 +/- 0.1	30.0 +/- 0.1	84.6 +/- 0.1	14.39 +/- 0.59	-37.96 +/- 1.54	23.33 +/- 0.69	0.62 +/- 0.04
V	15.0 +/- 0.1	30.0 +/- 0.1	85.2 +/- 0.1	19.35 +/- 0.64	-47.20 +/- 1.62	28.03 +/- 0.73	0.69 +/- 0.04
W	6.0 +/- 0.1	25.0 +/- 0.1	85.6 +/- 0.1	16.24 +/- 0.61	-43.40 +/- 1.60	26.22 +/- 0.71	0.62 +/- 0.04
X	9.9 +/- 0.1	25.0 +/- 0.1	83.0 +/- 0.1	19.30 +/- 0.64	-49.22 +/- 1.66	29.14 +/- 0.75	0.66 +/- 0.04
Y	10.0 +/- 0.1	35.0 +/- 0.1	84.5 +/- 0.1	8.56 +/- 0.54	-24.78 +/- 1.41	16.49 +/- 0.62	0.52 +/- 0.05
Z	15.1 +/- 0.1	35.0 +/- 0.1	85.5 +/- 0.1	13.60 +/- 0.59	-35.46 +/- 1.52	21.83 +/- 0.68	0.62 +/- 0.05

Fig. 2: Picture of the test bench

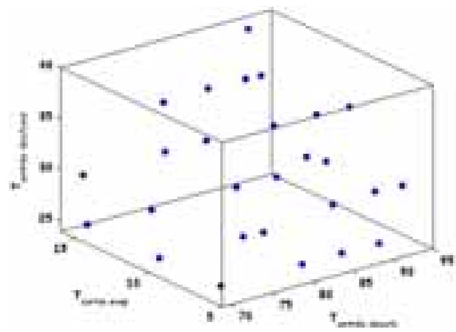

Fig. 3: Representation of the different selected tests in function of three working temperatures

4. Modelling and parameter identification

The physical model of absorption chiller [18] uses a properties library based on the work from Patek and Komflar [19]. To complete the ideal model detailed before, the heat exchanger technology must be integrated. An equation system is then added for each component (evaporator, condenser, absorber and desorber). Written in the case of the desorber, it gives to the heat transfer fluid and the heat exchanger:

$$\begin{cases} \dot{Q}_{desorb} = \dot{m}_{desorb} \cdot Cp_{eau} \cdot \left(T_{desorb\ outlet} - T_{desorb\ inlet}\right) \\ \dot{Q}_{desorb} = UA_{desorb} \cdot \Delta Tlm_{desorb} = UA_{desorb} \cdot \dfrac{T_{desorb\ inlet} - T_{desorb\ outlet}}{ln\left(\dfrac{T_{desorb\ inlet} - T_{desorb}}{T_{desorb\ oulet} - T_{desorb}}\right)} \end{cases} \quad (5)$$

But this technological integration introduces one design parameter by component, i.e. four UA factors representing the product between the global exchange coefficient and the exchange area. Two others are required to completely describe the machine: the diluted mass flow rate imposed by the pump and the efficiency of the internal heat exchanger.

Modeling the chiller requires to identify these unknowns. These sixth design parameters are determined thanks to the steady states tests of the previously part of this document. The method consists in the comparison between simulated results of the model and some experiments. 3 tests from the 27 of table 2 are selected (nomi, Q and Y) for the identification procedure and the chilling and heating power levels are used to minimize the criterion defined by:

$$MIN\left\{\sum_{n=1}^{n=3}\left[\left(\frac{\dot{Q}_{desorb\ meas\ n} - \dot{Q}_{desorb\ simul\ n}}{\dot{Q}_{desorb\ meas\ n}}\right)^2 + \left(\frac{\dot{Q}_{evap\ meas\ n} - \dot{Q}_{evap\ simul\ n}}{\dot{Q}_{evap\ meas\ n}}\right)^2\right]\right\} \quad (6)$$

The chosen identification method is the variable step simplex [20] and the results are presented in the table 2.

Table 2: Results of the parameter identification

UA_{evap}	UA_{desorb}	UA_{abs}	UA_{cond}	Diluted solution Flow rate $\dot{d}$	Thermal Efficiency ε
W/K	W/K	W/K	W/K	L/s	
3473	5339	4959	6390	0.12642	0.574

As the machine is relatively compact and as information about heat exchangers are relatively difficult to obtain or estimate, the obtained values are very delicate to interpret. So, to validate these identified parameters, the 24 other tests have been simulated and compared to the experiment. These comparisons are realized for the three powers (chilling, cooling and heating) and the associated COP. They are presented in the figure 4, 5, 6 and 7.

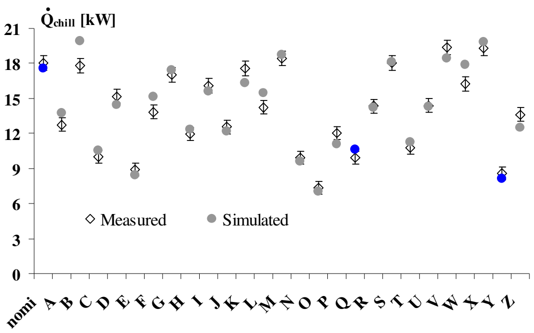

Fig. 4 - Comparison of the simulated and the experimental evaporating capacities.

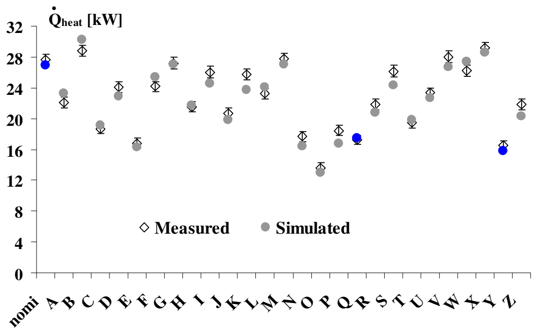

Fig. 5 - Comparison of the simulated and the experimental heating capacities.

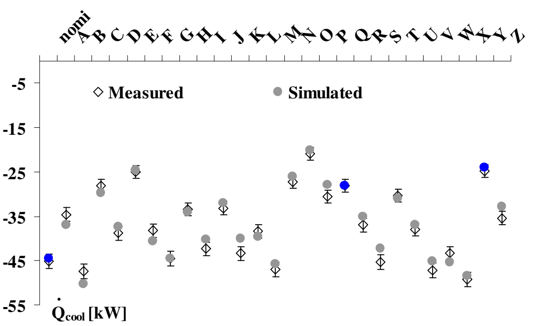

Fig. 6 - Comparison of the simulated and the experimental cooling powers.

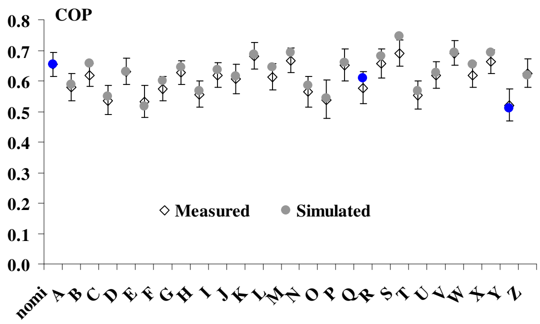

Fig. 7 - Comparison of the simulated and the experimental COP.

The results are very satisfying because the mean differences are only 4 % and in the uncertainty area for the highest majority of the 27 selected tests. So, the different powers and the associated COP are particularly well estimated by this model.

This chiller measures also the low and high pressure when working. The comparison between the simulated and the experiment for both pressures is represents in the figure 8 and 9.

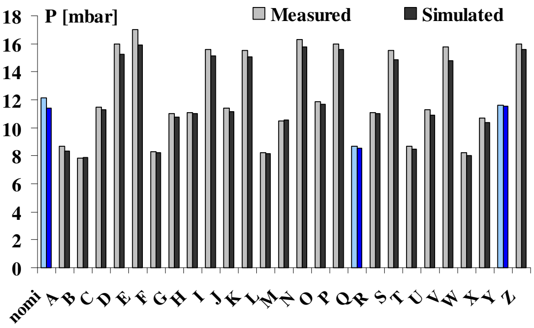

Fig. 8 - Comparison of the simulated and the experimental low pressures.

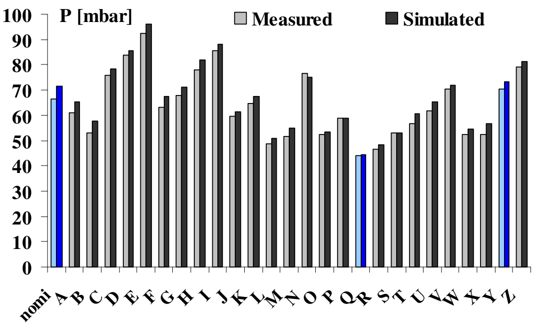

Fig. 9 - Comparison of the simulated and the experimental high pressures.

A good accuracy is observed between the simulated and measured pressures. The mean differences are only 3 % for the low pressure and 4 % for the high pressure.

5. Conclusion

The goal which consists in determining by identification some missing or inaccessible characteristic parameters of the studied absorption chiller is completed. The comparison, with the experiments in all other cases, shows the reliability and validity of the model. It is capable to evaluate the different power level as well as the COP of the chiller for a given triplet temperature, with an uncertainty of a few %. The model is also capable to evaluate the internal working pressures with a good accuracy.

Now, the identification procedure is validated on another chiller with this machine EAW which is distributed by SHÜCO. In a previous work, the method has been tested with ROTARTICA Solar 045 and the results were very satisfying [21, 22]. Soon a chiller SCHÜCO LB 30 will be modeled with the same identification tools.

References

[1] IPCC, 2001a. Climate Change 2001: The Scientific Basis. Technical Summary, Intergovernmental Panel on Climate Change. Cambridge University Press, Cambridge,

[2] Balaras C.A., Grossman G., Henning M., Infante Ferreira C.A., Podesser E., Wang L., Wiemken E., Solar air conditioning in Europe – an overview, Renewable and Sustainable Energy Reviews 11 (2007) 299-314,

[3] Mugnier D., Task 38 – Solar air-conditioning and refrigeration workshop, Solar Cooling Economics, Orlando, January 2010,

[4] Lamp P. and Ziegler F., European research on solar-assisted air conditioning, International Journal of Refrigeration 21 (1998) 89-99,

[5] Gershon Grossman, Solar-powered systems for cooling, dehumidification and air-conditioning, Solar Energy 72 (2002) 53-62,

[6] D.S. Kim and C.A. Infante Ferreira, Solar refrigeration options – a state-of-the-art review, International Journal of Refrigeration 31 (2008) 3-15,

[7] Wang R.Z., Ge T.S., Chen C.J., Ma Q.,Xiong Z.Q., Solar sorption cooling systems for residential applications: options and guidelines, International Journal of refrigeration 32 (2009) 638-660,

[8] Stephen White, State of the art in solar cooling, CSIRO Energy Technology, October 2009,

[9] Hans-Martin Henning, Solar assisted air conditioning of building – an overview, Applied Thermal Engineering 27 (2007) 1734-1749,

[10] Sparber W., Napolitano A., Melograno P., Overview on world wide installed solar cooling systems, 2nd International Conference Solar Air Conditioning, Tarragona – Spain, October 2007,

[11] Chen G., Hihara E., A new absorption refrigeration cycle using solar energy, Solar Energy 66 (1999) 479-482,

[12] Mateus T., Oliveira A.C.. Energy and economic analysis of an integrated solar absorption cooling and heating system in different building types and climates. Applied Energy 86 (2009) 949–957

[13] Nunez T., Design – state of the art, SOLATHERM Expert Mission, Tunis – Tunisia, December 2nd- 4th, 2008,

[14] Rotartica S.A., Rotartica product description, air conditioning appliances: solar line, single effect 4.5kW

[15] Izquierdo M., Lizarte R., Marcos J.D., Gutiérrez G., Air conditioning using an air-cooled single effect lithium bromide absorption chiller: Results of a trial conducted in Madrid in August 2005, Applied Thermal Engineering 28 (2008) 1074-1081,

[16] Rodriguez Hidalgo M.C., Rodriguez Aumente P., Izquierdo Millan M., Lecuona Neumann A., Salgado Mangual R., Energy and carbon savings in Spanish housing air-conditioning using solar driven absorption system, Applied Thermal Engineering 28 (2008) 1734-1744,

[17] Agyenim F., Knight I., Rhodes M., Design and experimental testing of the performance of an outdoor LiBr/H20 solar thermal absorption cooling system with a cold store, Solar Energy 84 (2010) 735-744,

[18] Castaing-Lasvignottes J., Belhani M., Strub F., Gibout S., Alaphilippe M. Modelisation and experimental validation of the unsteady behavior of a liquid absorption refrigeration machine. Application to solar external conditions. 3rd Int. Conf. on heat powered cycles Larnaca-Cyprus 11-13 October 2004

[19] Patek J., Klomfar J., A computationally effective formulation of the thermodynamic properties of the LiBr-/h2O solutions from 273 to 500 K over full composition range. International journal of refrigeration 29 (2006) 566-578,

[20] Walters, Parker, Morgan, Deming. Sequential simplex optimization. CRC press LLC 1991

[21] Chatagnon N., Bachmann M., Anies G. and Castaing-Lasvignottes J., Simulation of a domestic absorption chiller, 5th Francophone Colloquium in Energy, Environment, Economy and Thermodynamics, Iasi – Romania, 5-7 May 2010,

[22] Chatagnon N., Bachmann M., Anies G. and Castaing-Lasvignottes J., Analyse énergétique statique d'une machine à absorption solaire, Congrès Société Française de Thermique 2010, Le Touquet – France, 25-28 Mai 2010,

Acknowledgment

This work has been funded by the ADEME in an ANR Project ABCLIMSOL (PREBAT 2007).